Symmetry Protected Topological Phases

1 Introduction

In this lecture note, I will give a brief introduction to symmetry protected topological (SPT) phases in 1D, 2D, and 3D, through examples and concrete models.

Symmetry protected topological phases are gapped phases with certain global symmetry (time reversal, charge conjugation, discrete Z_N symmetry, spatial symmetry etc.). The ground state does not spontaneously break the symmetry and is unique on closed manifolds. On an open manifold on the other hand, the system has nontrivial edge modes (degenerate or gapless) such that there cannot be a unique gapped ground state.

The discovery of topological insulators and topological superconductors was a major breakthrough in the study of symmetry protected topological phases. Later, it was realized that such phenomena is not restricted to free fermion systems, but can be found in general interacting systems as well. A systematic study of interacting SPT phases followed, although the simplest interacting SPT model, the Haldane chain, has been known since the 1980s.

In this note, we introduce SPT phases following the historical path in the following steps:

1. Haldane phase in 1D
2. Topological insulator in 2D
3. Symmetry protected topological phase with Z_2 symmetry in 2D interacting bosonic systems
4. Duality between 2D SPT and gauge theory
5. Brief survey of SPT phases in various dimensions

2 Haldane phase in 1D

The spin 1 chain with anti-ferromagnetic Heisenberg interaction provides the first and simplest example of symmetry protected topological order. Consider the Hamiltonian

$$H = \sum_i \vec{S}_i \cdot \vec{S}_{i+1} \tag{1}$$

where $\vec{S}$ is the spin 1 operator

$$S^x = \frac{1}{\sqrt{2}} \begin{pmatrix} 0 & 1 & 0 \\ 1 & 0 & 1 \\ 0 & 1 & 0 \end{pmatrix}, S^y = \frac{i}{\sqrt{2}} \begin{pmatrix} 0 & -1 & 0 \\ 1 & 0 & -1 \\ 0 & 1 & 0 \end{pmatrix}, S^z = \begin{pmatrix} 1 & 0 & 0 \\ 0 & 0 & 0 \\ 0 & 0 & -1 \end{pmatrix} \tag{2}$$

This Hamiltonian has a rich symmetry, including spin rotation and time reversal ($\vec{S} \to -\vec{S}$).

What is the ground state like? For classical spin, anti-ferromagnetic interaction leads to Neel order, with spins ordered as $\uparrow\downarrow\uparrow\downarrow...$ In 1D quantum chains, long range order cannot survive and usually gets reduced to power law decaying correlation. This is what happens in anti-ferromagnetic Heisenberg spin 1/2 chain, which is known to be gapless. For the spin 1 chain, it was thought to be gapless as well until Haldane pointed that it should actually be gapped[9]. Moreover, as we are going to see below, it has symmetry protected topological order!

The Heisenberg model is very hard to solve and the existence of a gap remained a controversy for quite some time. On the other hand, exact ground state can be found for a slightly modified Hamiltonian proposed by Affleck, Kennedy, Lieb and Tasaki (AKLT) [1].

$$H = \sum_i \vec{S}_i \cdot \vec{S}_{i+1} + \frac{1}{3}\left(\vec{S}_i \cdot \vec{S}_{i+1}\right)^2 \tag{3}$$

By adding the quadratic interaction $\frac{1}{3}\left(\vec{S}_i \cdot \vec{S}_{i+1}\right)^2$, the Hamiltonian term becomes the projection to the total spin 2 sector for the two spin 1's at site i and $i+1$. That is to say, the total spin 2 sector has a higher energy, while the total spin 1 and total spin 0 sector has lower energy. Energy would be minimized if every pair of nearest neighbor spins satisfy this condition, i.e. if every pair of them has total spin 0 or 1 but not 2.

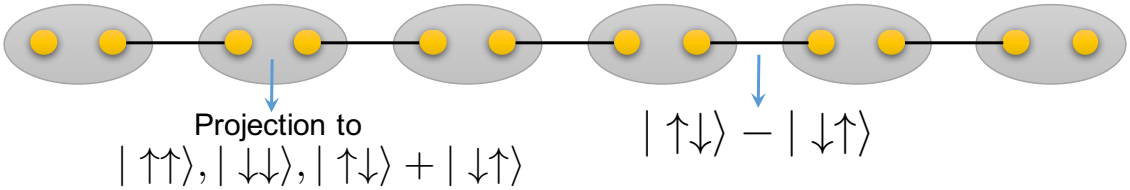

Figure 1: The valence bond ground state of the AKLT model. The spin 1 on each lattice site can be decomposed into two spin 1/2's which form singlets between nearest neighbor pairs. At the two ends of an open chain, there are two isolated spin 1/2's giving rise to a four fold ground state degeneracy.

This condition can indeed be satisfied. As shown in Fig.1, consider each spin 1 (grey oval) as composed of two spin 1/2's (yellow circle). Put the right spin 1/2 on site i and the left spin 1/2 on site $i+1$ into a singlet state $|\uparrow\downarrow\rangle - |\downarrow\uparrow\rangle$. Now among the four spin 1/2's on site i and $i+1$, two of them has total spin 0, therefore the total spin of the four can only be either 0 or 1. In this way we have found the ground state of Eq. 3. The full wave function can be written as

$$|\psi_{AKLT}\rangle = \prod_i P_1^i \prod_{i,i+1} \frac{1}{\sqrt{2}}\left(|\uparrow_r^i\downarrow_l^{i+1}\rangle - |\downarrow_r^i\uparrow_l^{i+1}\rangle\right) \tag{4}$$

where $P_1^i = |1\rangle\langle\uparrow_l^i\uparrow_r^i| + |-1\rangle\langle\downarrow_l^i\downarrow_r^i| + \frac{1}{\sqrt{2}}|0\rangle\left(\langle\uparrow_l^i\downarrow_r^i| + \langle\downarrow_l^i\uparrow_r^i|\right)$ is the projection from two spin 1/2's back to the spin 1 basis.

This wave function is called a 'Valence Bond Solid'. In 1, it was shown that this wave function has a finite correlation length. That is

$$\langle\psi_{AKLT}|O_iO_j|\psi_{AKLT}\rangle - \langle\psi_{AKLT}|O_i|\psi_{AKLT}\rangle\langle\psi_{AKLT}|O_j|\psi_{AKLT}\rangle \sim e^{-|i-j|/\xi} \tag{5}$$

where ξ is the correlation length. Moreover, the excitations on top of this ground state wave function consist of flipping the singlets into triplets and cost finite energy. Therefore, the ground state is gapped and is very different from the spin 1/2 case.

From this valence bond structure of the wave function, it is easy to see the nontrivial SPT order. On a closed ring with periodic boundary condition, all the spin 1/2's are paired up and the ground state is unique. It is invariant under both spin rotation ($\prod_i e^{i\vec{\theta}\vec{S}_i}$) and time reversal ($\prod_i e^{i\pi S_i^y} K$, where K is complex conjugation). There is no spontaneous symmetry breaking, yet the unique gapped ground state has a nontrivial order.

To see this, notice that on an open chain, the spin 1/2's at the two ends of the chain are far away from each other and hence not coupled. They can point in any direction without affecting the energy (in the thermodynamic limit). Therefore, the ground state is 4 fold degenerate, with each spin 1/2 contributing 2 fold degeneracy. If spin rotation or time reversal symmetry is broken by adding, e.g., a magnetic field, the edge spin is polarized and the degeneracy is lifted. If either spin rotation or time reversal is preserved, the degeneracy is always robust and is a signature of the symmetry protected topological order in the AKLT model.

Such a statement holds not only for the AKLT mode, but for all models in the same phase (supposedly including the Heiserberg model Eq. 1). If we vary the model within the phase, the edge state might change. For example, it might gets wider and changes from a spin 1/2 to a spin 3/2 by involving the neighboring spin 1. However, as long as it is a half integer spin, it always has a nontrivial degeneracy, indicating the nontrivial SPT order.

This is related to a special property of the half integer spins as compared to integer spins under spin rotation or time reversal symmetry. A half integer spin transforms under 2π spin rotation as $e^{i2\pi\sigma^{\vec{n}}} = -1$ while an integer spin transforms under 2π rotation as $e^{i2\pi S^{\vec{n}}} = 1$. Therefore, these two cases cannot be smoothly connected. In particular, a half integer spin edge state cannot become a zero spin edge state which has no degeneracy. On the other hand, a integer spin can be connected to spin 0, hence removing the degeneracy.

Similarly under time reversal symmetry, a half integer spin transforms as $T^2 = e^{i\pi\sigma^y} K e^{i\pi\sigma^y} K = -1$ while an integer spin transforms as $T^2 = e^{i\pi S^y} K e^{i\pi S^y} K = 1$. Therefore integers spins and half integer spins are fundamentally different under time reversal symmetry. And the edge state cannot change from one to another without a phase transition.

Spin 1/2 under spin rotation and time reversal symmetry provides a prototypical example of a projective representation of symmetry. In general, for a symmetry group G, a usual representation consists of matrices $M(g), g \in G$, which satisfy

$$M(g_1)M(g_2) = M(g_1 g_2) \tag{6}$$

A projective representation consists of matrices $M(g), g \in G$ which satisfy

$$M(g_1)M(g_2) = \omega(g_1, g_2)M(g_1 g_2) \tag{7}$$

for some phase factor $\omega(g_1, g_2) \neq 1$. The ω's have to satisfy

$$\omega(g_1, g_2)\omega(g_1 g_2, g_3) = \omega^{s_1}(g_2, g_3)\omega(g_1, g_2 g_3) \tag{8}$$

where $s_1 = 1$ if g_1 is unitary symmetry, $s_1 = -1$ if g_1 is anti-unitary (involves time reversal). On the other hand, one can redefine the phase factor of $M(g)$ by $\alpha(g)$. Therefore, any two sets of ω's related by

$$\tilde{\omega}(g_1, g_2) = \omega(g_1, g_2)\frac{\alpha(g_1)\alpha^{s_1}(g_2)}{\alpha(g_1 g_2)} \tag{9}$$

are considered equivalent. Eq. 8 and 9 lead to a classification of projective representations for symmetry group G. In particular, for spin rotation $G = SO(3)$, there are two classes and for time reversal there are two classes. Spin 1/2 corresponds to the nontrivial class in both cases.

This discussion of projective representation is important for the study of SPT phases because it has been shown[21, 26, 5, 24] that there is a one to one correspondence between one dimensional bosonic SPT phases with symmetry G and equivalence class of projective representations of group G.

3 Topological insulator in 2D

While in 1D, SPT phases were first discovered in spin chains, in 2D they were discovered in a very different system – electronic insulators. We are going to introduce the idea of topological insulator in 2D[14, 15, 17] in this section and discuss its relation to the Haldane chain.

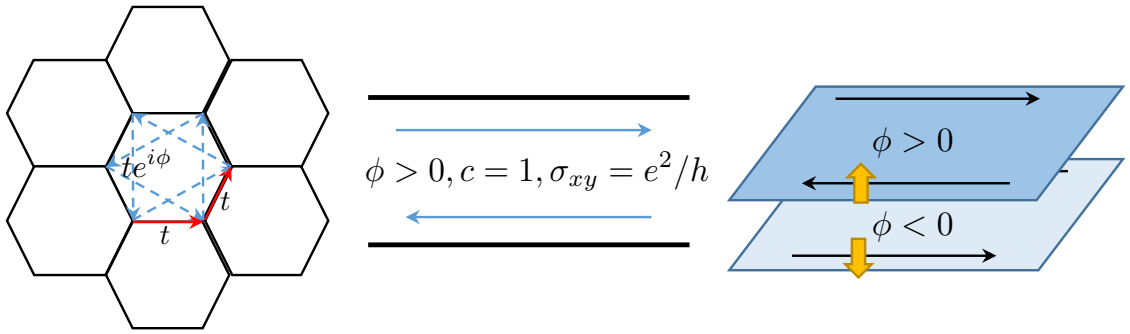

Figure 2: Left: Haldane model (of hopping electrons) on a honeycomb lattice. Middle: Edge mode and Hall conductance of the Haldane model. Right: Stacking two copies of the Haldane model, one with spin up and Chern number 1 and one with spin down and Chern number -1, gives rise to the topological insulator.

To introduce topological insulator, we are going to start from another Haldane model. Consider a 2D honeycomb lattice as shown in Fig.2 where each lattice site contains one electron orbit. The electrons can hop from one site to another. If the electrons only hop between nearest neighbor sites with real hopping coefficient, the band structure is gapless. If next nearest neighbor hopping is added with a complex phase factor ϕ, as shown in Fig.2, time reversal symmetry is broken and a gap opens up.

The band structure that results has a nontrivial Chern number ($c = 1$) and because of that a nontrivial edge state. That is, on a closed manifold, the band is completely gapped but it becomes gapless if the manifold has a boundary and the gapless modes live near the edge. On a strip geometry, there are left moving gapless modes Ψ_L near the lower edge of the system and right moving gapless modes Ψ_R near the upper edge of the system. The low energy theory of the two edges can be described as

$$H = vk(\Psi^\dagger_{Lk}\Psi_{Lk} - \Psi^\dagger_{Rk}\Psi_{Rk}) \tag{10}$$

The edge state gives rise to a quantized Hall conductance $\sigma_{xy} = e^2/h$. If ϕ goes to $-\phi$, the Chern number gets a minus sign and the Hall conductance also gets a minus sign.

Now consider two species of electrons, one with spin up $\uparrow$, one with spin down $\downarrow$. The electrons

hop on the honeycomb lattice such that the up spins hop with a phase factor of ϕ and the down spins hop with a phase factor of $-\phi$. Spin is preserved during the hopping process. Therefore, the system effectively consists of two layers – a spin up layer and a spin down layer, one with $c = 1$ and $\sigma_{xy} = e^2/h$ and one with $c = -1$ and $\sigma_{xy} = -e^2/h$, as shown in Fig.2. The fact that the hopping phase factor is spin dependent comes from the spin orbital coupling of the electron.

There are then two gapless modes near the edge. For example, along the upper edge, there is a right moving mode of spin up electrons $\Psi_{R\uparrow}$ and a left moving mode of spin down electrons $\Psi_{L\downarrow}$. The low energy effective Hamiltonian along the upper edge reads

$$H_u = vk(\Psi^\dagger_{L\downarrow k}\Psi_{L\downarrow k} - \Psi^\dagger_{R\uparrow k}\Psi_{R\uparrow k}) \tag{11}$$

This is the so called helical edge mode of topological insulator.

When both the right moving and left moving modes are present near one edge, it is possible to induce tunneling between the two modes by adding terms like

$$m\left(\Psi^\dagger_{L\downarrow k}\Psi_{R\uparrow k} + \Psi^\dagger_{R\uparrow k}\Psi_{L\downarrow k}\right) \tag{12}$$

The energy of the edge modes becomes $\epsilon(k) = \pm\sqrt{(vk)^2 + m^2}$ and a gap opens.

However, if time reversal symmetry is preserved, then this term is not allowed. Because under the time reversal transformation

$$\Psi_{R\uparrow k} \to \Psi_{L\downarrow -k}, \Psi_{L\downarrow k} \to -\Psi_{R\uparrow -k} \tag{13}$$

The tunneling term obtains a minus sign. Therefore, the edge state remains gapless when time reversal symmetry is preserved.

In fact, there is another way to open up a gap on the edge, by inducing superconductivity. If pairing terms like

$$\Delta\left(\Psi^\dagger_{L\downarrow k}\Psi^\dagger_{R\uparrow -k} + \Psi_{R\uparrow -k}\Psi_{L\downarrow k}\right) \tag{14}$$

are added to the edge, this again opens up a gap. While this term is time reversal invariant, it violates charge conservation symmetry. Therefore, the gapless-ness of the edge state is protected by both the charge conservation and the time reversal symmetry. If either is broken, then the edge can be gapped.

This is the basic story of topological insulator in 2D. It looks very different from the Haldane chain model we discussed in the previous section. One is a free fermion electronic insulator while the other is an interacting spin chain. However, if we think of their property in a more general sense, they are closely related. Let's compare them in the following table.

Comparison	Haldane Chain	Topological Insulator
Gap in the bulk	✓	✓
No fractional excitation in the bulk	✓	✓
No spontaneous symmetry breaking in the bulk	✓	✓
Gapless / degenerate edge	spin 1/2	helical edge
Edge state protected by symmetry	spin rotation or time reversal	charge conservation and time reversal

Therefore, in this sense, Haldane chain and topological insulator both have symmetry protected topological order.

4 Z_2 SPT in 2D

Are there symmetry protected topological phases in interacting spin models of two and higher dimensions? In this section, we introduce the CZX model of interacting spins which has nontrivial SPT order protected by on-site Z_2 symmetry. Discussion in this section follows that in Ref.[5].

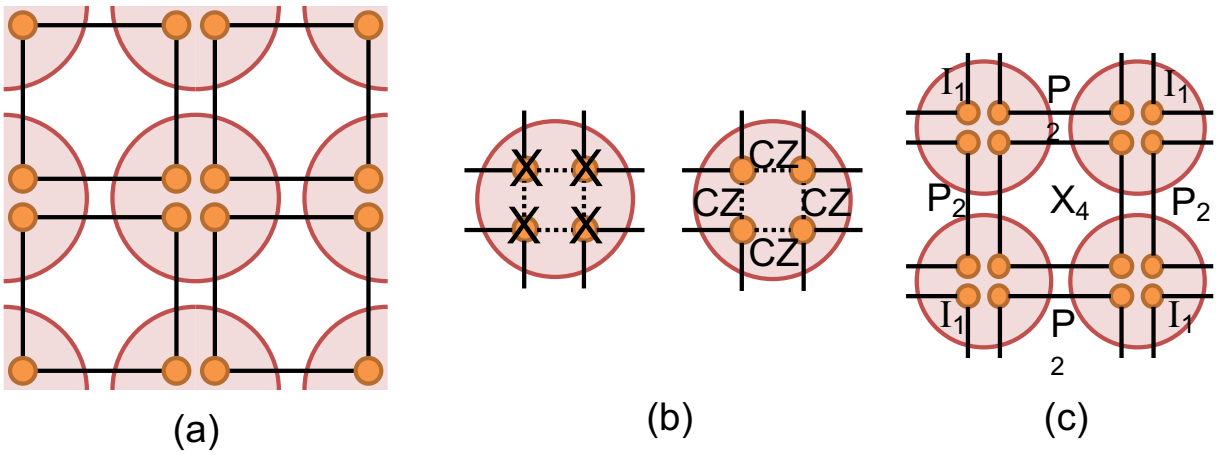

Figure 3: CZX model (a) each site (circle) contains four spins (dots) and the spins in the same plaquette (square) are entangled. (b) on-site Z_2 symmetry is generated by $U_{CZX} = X_1X_2X_3X_4CZ_{12}CZ_{23}CZ_{34}CZ_{41}$ (c) a local term in the Hamiltonian, which is a tensor product of one X_4 term and four P_2 terms as defined in the main text.

Consider a square lattice with four two-level spins per site, as shown in Fig. 3(a) where sites are represented by circles and spins are represented by dots. We denote the two levels as $|0\rangle$ and $|1\rangle$. The system has an on-site Z_2 symmetry as given in Fig. 3(b). It is generated by

$$U_{CZX} = U_X U_{CZ} \tag{15}$$

where

$$U_X = X_1 \otimes X_2 \otimes X_3 \otimes X_4 \tag{16}$$

X_i is Pauli X operator on the ith spin and

$$U_{CZ} = CZ_{12}CZ_{23}CZ_{34}CZ_{41} \tag{17}$$

where CZ is the controlled-Z operator on two spins defined as

$$CZ = |00\rangle\langle 00| + |01\rangle\langle 01| + |10\rangle\langle 10| - |11\rangle\langle 11| \tag{18}$$

As defined, CZ does nothing if at least one of the spins is in state $|0\rangle$ and it adds a minus sign if both spins are in state $|1\rangle$. Different CZ operators overlap with each other. But because they commute, U_{CZ} is well defined. Note that U_{CZ} cannot be decomposed into separate operations on the four spins and the same is true for U_{CZX}. U_X and U_{CZ} both square to I and they commute with each other. Therefore, U_{CZX} generates a Z_2 group.

The Hamiltonian of the system is defined as a sum of local terms around each plaquette. Plaquettes are represented by squares in Fig. 3. $H = \sum H_{p_i}$, where the term around the ith plaquette H_{p_i}

acts not only on the four spins in the plaquette but also on the eight spins in the four neighboring half plaquettes as shown in Fig. 3(c)

$$H_{p_i} = -X_4 \otimes P_2^u \otimes P_2^d \otimes P_2^l \otimes P_2^r \tag{19}$$

where X_4 acts on the four spins in the middle plaquette as

$$X_4 = |0000\rangle\langle 1111| + |1111\rangle\langle 0000| \tag{20}$$

and P_2 acts on the two spins in every neighboring half plaquette as

$$P_2 = |00\rangle\langle 00| + |11\rangle\langle 11| \tag{21}$$

P_2^u, P_2^d, P_2^l, P_2^r acts on the up, down, left and right neighboring half plaquettes respectively. For the remaining four spins at the corner, H_{p_i} acts as identity on them. The P_2 factors ensure that each term in the Hamiltonian satisfies the on-site Z_2 symmetry defined before.

All the local terms in the Hamiltonian commute with each other, therefore it is easy to solve for the ground state. If the system is defined on a closed surface, it has a unique ground state which is gapped. In the ground state, every four spins around a plaquette are entangled in the state

$$|\psi_{p_i}\rangle = |0000\rangle + |1111\rangle \tag{22}$$

and the total wavefunction is a product of all plaquette wavefunction. If we allow any local unitary transformation, it is easy to see that the ground state can be disentangled into a product state, just by disentangling each plaquette separately into individual spin states. Therefore, the ground state is short range entangled. However, no matter what local unitary transformations we apply to disentangle the plaquettes, they necessarily violate the on-site symmetry and in fact, the plaquettes cannot be disentangled if the Z_2 symmetry is preserved, due to the nontrivial SPT order of this model which we show below.

First let's check that this ground state is indeed invariant under the on-site Z_2 symmetry. Obviously this state is invariant under U_X applied to every site. It is also invariant under U_{CZ} applied to every site. To see this note that between every two neighboring plaquettes, CZ is applied twice, at the two ends of the link along which they meet. Because the spins within each plaquette are perfectly correlated (they are all $|0\rangle$ or all $|1\rangle$), the effect of the two CZ's cancel each other, leaving the total state invariant.

Therefore, we have introduced a 2D model with on-site Z_2 symmetry whose ground state does not break the symmetry and is short-range entangled. We can add small perturbation to the system which satisfies the symmetry and the system is going to remain gapped and the ground state short range entangled and symmetric. It seems that the system is quite trivial and boring. However, we are going to show that surprising things happen if the system has a boundary and because of these special features the system cannot be smoothly connected to a trivial phase as long as global Z_2 symmetry is preserved.

The non-trivialness of this model shows up on the boundary. Suppose that we take a simply connected disk from the lattice, as shown in Fig.4(a).

The reduced density matrix of spins in this region is invariant under on-site symmetry in this region. The reduced density matrix is a tensor product of individual terms on each full plaquette, half plaquette and corner of plaquette respectively. On a full plaquette

$$\rho_4 = (|0000\rangle + |1111\rangle)(\langle 0000| + \langle 1111|) \tag{23}$$

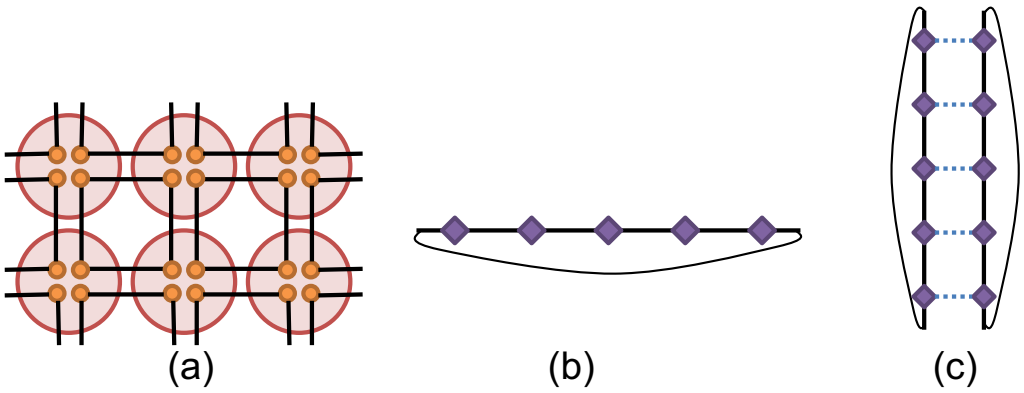

Figure 4: (a)CZX model on a disk with boundary (b) boundary effective degrees of freedom form a 1D chain which cannot have a short range entangled symmetric state (c) two boundaries together can have a short range entangled symmetric state which is a product of entangled pairs between effective spins connected by a dashed line.

On a half plaquette

$$\rho_2 = |00\rangle\langle 00| + |11\rangle\langle 11| \tag{24}$$

On a corner of a plaquette

$$\rho_1 = |0\rangle\langle 0| + |1\rangle\langle 1| \tag{25}$$

The state of spins on the plaquettes totally inside this region is completely fixed. But on the boundary there are free degrees of freedom. However, only part of the total Hilbert space of the spins on the boundary is free. In particular, two spins in a half plaquette on the boundary are constrained to the two-dimensional subspace $|00\rangle\langle 00| + |11\rangle\langle 11|$ and form an effective spin degree of freedom if we map $|00\rangle$ to $|\tilde{0}\rangle$ and $|11\rangle$ to $|\tilde{1}\rangle$.

In Fig. 4(b), we show the effective degrees of freedom on the boundary as diamonds on a line. Projecting the total symmetry operation on the disk to the support space of the reduced density matrix, we find that the effective symmetry operation on the boundary effective spins is $\tilde{U}_{CZX} = \prod_{i=1}^{N} \tilde{X}_i \prod_{i=1}^{N} \tilde{CZ}_{i,i+1}$, with Pauli $\tilde{X}$ on each effect spin and $\tilde{CZ}$ operation between neighboring effective spins. The boundary is periodic and $\tilde{CZ}_{N,N+1}$ acts on effective spin N and 1. This operator generates a Z_2 symmetry group.

This is a very special symmetry on a 1D system. First it is not an on-site symmetry. In fact, no matter how we locally group sites and take projections, the symmetry operations are not going to break down into an on-site form. Moreover, no matter what interactions we add to the boundary, as long as it preserves the symmetry, the boundary cannot have a gapped symmetric ground state. To see this, we are going to consider some simple cases.

The simplest interaction term preserving this symmetry is $Z_i Z_{i+1}$. This is an Ising interaction term and its ground state spontaneously breaks the Z_2 symmetry. In the transverse Ising model, the system goes to a symmetric phase if magnetic field in the x direction is increased. However, X_i breaks the Z_2 symmetry $\tilde{U}_{CZX}$ on the boundary and therefore cannot be added to the Hamiltonian. One can instead symmetrize the term and obtain $X_i + Z_{i-1} X_i Z_{i+1}$. If one tries to solve this Hamiltonian, one would find that it is gapless. In particular, the gapless edge state can be described

as a free boson model with Lagrangian

$$\mathcal{L}_e = \frac{1}{4\pi}\partial_x\phi_1\partial_t\phi_2 + \partial_x\phi_2\partial_t\phi_1 \tag{26}$$

where ϕ_1 and ϕ_2 are 2π periodic scalar fields. The global Z_2 symmetry acts effectively as

$$\phi_1 \to \phi_1 + \pi, \phi_2 \to \phi_2 + \pi \tag{27}$$

Due to the nontrivial symmetry action on both ϕ_1 and ϕ_2, usual gapping terms for this boson theory $\cos(\phi_1)$ and $\cos(\phi_2)$ cannot be added and the edge state remains gapless as long as symmetry is not broken.

The special property on the boundary only shows up when there is an isolated single boundary. If we put two such boundaries together and allow interactions between them, everything is back to normal. As shown in Fig.4(c), if we have two boundaries together, there is indeed a short range entangled symmetric state on the two boundaries. The state is a product of entangled pairs of effective spins connected by a dashed line. The entangled pair can be chosen as $|\tilde{0}\tilde{0}\rangle + |\tilde{1}\tilde{1}\rangle$. In contrast to the single boundary case, we can locally project the two effective spins connected by a dashed line to the subspace $|\tilde{0}\tilde{0}\rangle\langle\tilde{0}\tilde{0}| + |\tilde{1}\tilde{1}\rangle\langle\tilde{1}\tilde{1}|$ and on this subspace, the symmetry acts in an on-site fashion.

This result should be expected because if we have two pieces of sheet with boundary and glue them back into a surface without boundary, we should have the original short range entangled 2D state back. Indeed if we map the effective spins back to the original degrees of freedom $|\tilde{0}\rangle \to |00\rangle$ and $|\tilde{1}\rangle \to |11\rangle$, we see that the short range entangled state between two boundaries is just the a chain of plaquettes $|0000\rangle + |1111\rangle$ in the original state.

This model serves as an example of non-trivial SPT order in 2D short range entangled states that only needs to be protected by on-site symmetry. In the above discussion, we demonstrated the nontrivial-ness of the edge state by looking at particular realizations of the edge Hamiltonian. In [5], we prove, using the Matrix Product University Operator formalism, that the edge cannot be in a short range entangled state without breaking symmetry.

5 Duality between 2D SPT and gauge theory

Besides looking at the edge, a powerful way to detect SPT order with unitary symmetries in two and higher dimensions is to map them to the corresponding gauge theories. In particular, the duality transformations between Z_2 SPT phases in 2D and Z_2 gauge theories in 2D can be used to distinguish the SPT phases from the braiding statistics of the gauge fluxes. In this section, we are going to explain this connection using a different lattice realization of Z_2 SPT order in 2D. Discussion in this section follows that in [18].

Consider first the Ising symmetric phase with one spin 1/2 per each plaquette of the honeycomb lattice, as shown in Fig.5 (a). The Hamiltonian takes the simple form

$$H^0 = -\sum_a \sigma_a^x \tag{28}$$

and the ground state is simply a product of $\frac{1}{\sqrt{2}}(|\uparrow\rangle + |\downarrow\rangle)$ on each plaquette. This Hamiltonian is invariant under the global Z_2 symmetry of $\prod_a \sigma_a^x$. If we think of the $|\uparrow\rangle$ state as one Z_2 domain

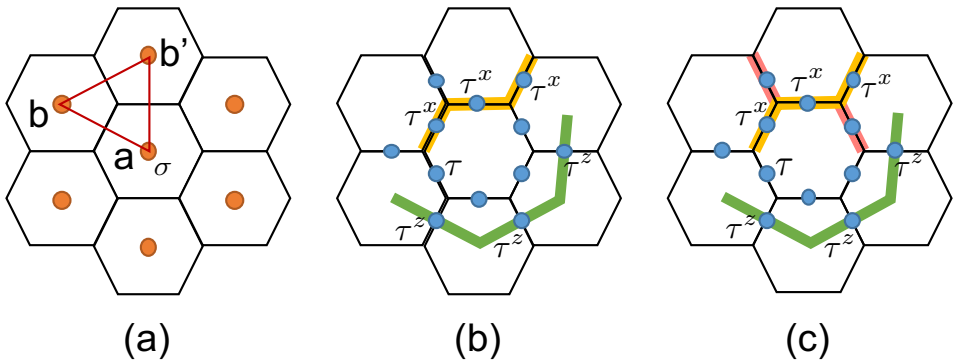

Figure 5: (a) Z_2 symmetric model with one σ spin per plaquette on the honeycomb lattice representing the Z_2 domains. (b) String operator for creating gauge charge and gauge flux in H_g^0. (c) String operator for creating gauge charge and gauge flux in H_g^1.

and the $|\downarrow\rangle$ state as the opposite domain, then the ground state is an equal weight superposition over all domain configurations.

$$|\psi^0\rangle = \sum_D |D\rangle \tag{29}$$

where D labels domain configurations.

A duality transformation maps this Z_2 symmetric phase to the Z_2 gauge theory. Introduce degree of freedom τ on the edges of the honeycomb lattice. The domain degrees of freedom σ can be mapped to the domain wall degrees of freedom τ by requiring that

$$\tau_{ab}^z = \sigma_a^z \sigma_b^z \tag{30}$$

where a, b label neighboring plaquettes. Because of this mapping, the τ spins naturally satisfy the constraint

$$\tau_{ab}^z \tau_{bc}^z \tau_{ca}^z = 1 \tag{31}$$

The σ_a^x term, which flips the domain in each plaquette, is now mapped to $\prod_b \tau_{ab}^x$ where the product is over all neighboring plaquettes b of plaquette a. Combining this term together with the constraint term, we get the Hamiltonian for the Z_2 gauge theory

$$H_g^0 = -\sum_v \prod_{e \in v} \tau_e^z - \sum_p \prod_{e \in p} \tau_e^x \tag{32}$$

where the first sum is over all vertices v and each terms involves the product over all edges e terminating at the vertex v, the second sum is over all plaquettes p and each term involves the product over all edges e bounding the plaquette p. The ground state is an equal weight superposition of all domain wall configurations.

$$|\psi^0\rangle = \sum_C |C\rangle \tag{33}$$

where C labels domain configurations.

While there seems to be a straight forward mapping between domain configurations and domain wall configurations, they are fundamentally different which shows up on manifolds with nontrivial topology, like a torus. On a torus, every domain configuration can be mapped to a domain wall configuration, but not every domain wall configuration can be mapped back to domains. In

particular, there can be nontrivial loops along the two big circles of the torus in the domain wall configuration, which does not bound any region on the torus, hence does not map to any domain configuration. As the nontrivial loops cannot be detected from local energetics, they contribute to ground state degeneracy on the torus and the Z_2 gauge theory is hence four fold degenerate on a torus while the Ising symmetric phase is not degenerate.

The above Hamiltonian is the standard Toric Code Hamiltonian on a honeycomb lattice. Unlike SPT phases, it has fractional excitations in the bulk and hence the kind of topological order that does not need symmetry protection. This type of topological order is usually called intrinsic and the system is said to have long-rang entanglement. The fractional excitations include the gauge charge e, the gauge flux m and their composite. The gauge charge e can be created in pairs with string operator $\tau^z\tau^z\tau^z...$ and the gauge flux m can be created in pairs with string operator $\tau^x\tau^x\tau^x...$ as shown in Fig.5 (b).

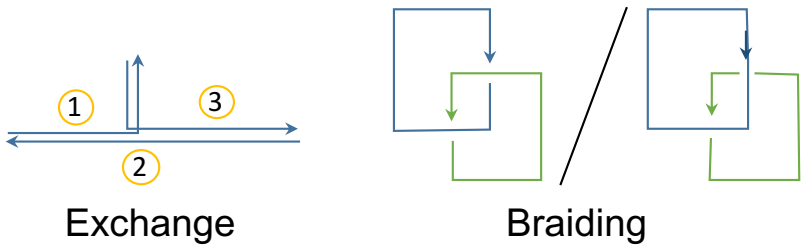

Figure 6: String operator configurations for calculating the topological spin and braiding statistics of fractional excitations. In the exchange subfigure, the arrows in the horizontal directions are on top of each other, although we shifted them to show their time dependence; the same is true for the vertical arrows.

The statistics of the fractional excitations can be read from the self commutation and mutual commutation relations of the string operators. In particular, the topological spin of a fractional excitation can be obtained by calculating the phase factor resulting from applying the string operator as shown in Fig.6 (a). Note that the arrows in the horizontal directions are on top of each other, although we shifted them to show their time dependence; the same is true for the vertical arrows. It is straight forward to see that both the $\tau^z\tau^z\tau^z...$ and $\tau^x\tau^x\tau^x...$ string operator give a phase factor of 1 in this process, indicating that both e and m are bosonic fractional excitations. The mutual braiding statistics of two fractional excitations can be calculated using the diagram in Fig.6 (b). The braiding phase factor basically comes from the commutation of the two string operators and for the e and m excitations, it is -1.

Now consider a different model with Z_2 global symmetry defined for the σ spins.

$$H^1 = \sum_a \sigma_a^x \prod_{<abb'>} i^{\frac{1-\sigma_b^z\sigma_{b'}^z}{2}} \tag{34}$$

where the product is over all nearest neighbor triangle of plaquettes involving plaquette a, as shown in Fig.5 (a). This Hamiltonian is again invariant under the Z_2 symmetry $\prod_a \sigma_a^x$. It can be checked that different terms in the Hamiltonian commute and the ground state can be found exactly. It may not be immediately obvious, but the ground state is again a superposition over all domain configurations but with phase factors. In particular, the configuration gets a -1 sign if there are an odd number of domain wall loops between domains.

$$|\psi^1\rangle = \sum_D (-1)^{N(D)}|D\rangle \tag{35}$$

where D labels domain configurations and $N(D)$ is the number of domain wall loops in this domain configuration.

H^1 is a model with nontrivial Z_2 SPT order, similar to the CZX model discussed above. One way to see its nontrivial SPT order is by looking at the edge states, as we did in the CZX case[18]. Here instead we are going to use the 'braiding statistics approach' discussed in [18]. In particular, we are going to show that the duality transformation maps H^1 to a different Z_2 gauge theory than that of H^0, demonstrating the nontrivial-ness of the SPT order in H^1.

Now apply the duality transformation as described above to H^1 by mapping the Z_2 domain degrees of freedom σ to Z_2 domain wall degrees of freedom τ as

$$\tau^z_{ab} = \sigma^z_a \sigma^z_b \tag{36}$$

The same constrain applies

$$\tau^z_{ab}\tau^z_{bc}\tau^z_{ca} = 1 \tag{37}$$

The terms in the Hamiltonian get mapped to $\prod_b \tau^x_{ab} \prod_{<abb'>} i^{\frac{1-\tau^z_{bb'}}{2}}$ and put together the full Hamiltonian of the Z_2 gauge theory is

$$H^1_g = -\sum_v \prod_{e\in v} \tau^z_e + \sum_p \prod_{e\in p} \tau^x_e \prod_{e\in \text{legs of } p} i^{\frac{1-\tau^z_e}{2}} \tag{38}$$

This is the Hamiltonian of the 'twisted' Z_2 gauge theory. While the Hamiltonian looks complicated, the ground state has a simple form, which can be deduced from the duality mapping. The ground state is a superposition of all domain wall configurations, with each domain wall loop carrying a phase factor of -1.

$$|\psi^1\rangle = \sum_C (-1)^{N(C)} |C\rangle \tag{39}$$

where C labels domain wall configurations and $N(C)$ is the number of domain wall loops in this domain wall configuration. Note that here $N(C)$ counts only the domain wall loops that bound a domain. On a torus, not every loop configuration bounds a domain. In particular, those along the nontrivial cycles of the torus do not. We have the choice of having them or not having them in the ground state wave function and superposing them with different weights. This freedom gives rise to the four fold ground state degeneracy on the torus, similar to the Toric Code case.

On the other hand, H^1_g represents a different kind of Z_2 gauge theory than the Toric Code as its fractional excitations have different statistics. The string operators that create such quasiparticle excitations are as shown in Fig.5 (c). The gauge charge is still created by $\tau^z\tau^z\tau^z...$ which commutes with every term of the Hamiltonian except the two plaquette terms at the end. On the other hand, the $\tau^x\tau^x\tau^x...$ operator, which creates gauge flux excitations in the Toric Code model, violates plaquette terms along its length in H^1_g. Therefore, it is not a string operator for deconfined excitations any more. It can be modified in such a way that it commutes with all the Hamiltonian terms along its length. In Fig.5 (c), we illustrate the modification by marking the edges adjacent to the string with red, indicating that there are non-trivial actions on the domain wall degrees of freedom on those edges. The extra nontrivial action is some phase factor in τ^z basis depending on the degrees of freedom both along the path and on the adjacent edges.

The change in string operator leads to the change in fractional statistics. The topological spin of the gauge charge remains the same, as the $\tau^z\tau^z\tau^z...$ operator remains the same. That is, the gauge charge is a boson. The braiding statistics of -1 between the gauge charge and the gauge flux is

still the same, as the $\tau^z\tau^z\tau^z$... operator and the modified gauge flux string operator, which involves $\tau^x\tau^x\tau^x$... and some phase factors still anti-commute with each other. However, the topological spin of the gauge flux can change due to the change in its string operator. Of course, without specifying the exact form of the new string operator, we cannot calculate explicitly the resulting statistics according to Fig.6 (exchange). We are not going to do this in this note, but only state that the topological spin turns out to be i for the gauge flux excitation of H_g^1.

Therefore, H_g^0 and H_g^1 represent two different types of Z_2 gauge theories. They both contain gauge charge excitations which are bosonic and gauge flux excitations which braiding with the gauge charges with a -1 phase factor. However, the gauge flux excitations is a boson for H_g^0 and a semion for H_g^1. There are the two, and the only two, distinct types of Z_2 gauge theory with bosonic gauge charge in $2D$. Correspondingly, H^0 and H^1 corresponds to two different SPT phases with Z_2 global symmetry. Here we are using a claim that two models with the same global symmetry correspond to different SPT phases if their dual gauge theory have different topological order (have different statistics). More detailed discussion of this relation and of the relevant models can be found in [18].

6 Brief survey of SPTs in various dimensions

We conclude this note with a brief survey of interesting SPT phases in various dimensions.

1. In 1D, the Haldane chain model illustrates the key feature of SPT phases – degenerate edge state forming a projective representation of the symmetry. Moreover, it provides prototypical example for nontrivial SPT phases with simple and important symmetries: time reversal, $SO(3)$ spin rotation, and discrete $Z_2 \times Z_2$ spin rotation (π rotation along x, y and z direction). With other symmetries, it is possible to have more varieties of SPT phases in spin / boson systems, but the key property of degenerate edge mode with projective representation remains the same.

2. In 1D fermion system, a topological phase with very similar structure exists – the Majorana chain model introduced by Kitaev[16]. The Majorana chain model does not belong to the class of SPT phases because its topological order does not require symmetry protection, but its ground state has a very similar structure to that of the AKLT model and I would like to discuss it briefly.

   The Majorana chain model exists in a 1D fermion chain with fermion creation and annihilation operators $c_k^\dagger$ and c_k. One such complex fermion mode can be decomposed into two Majorana modes with Majorana operators

   $$\gamma_{2k-1} = c_k^\dagger + c_k, \gamma_{2k} = i(c_k^\dagger - c_k) \tag{40}$$

   which satisfies $\gamma^2 = 1$, $\{\gamma_i, \gamma_j\} = 1$. Of course, this is just a mapping of operators in the system and it can be applied to any fermion Hamiltonian. One special feature of this mapping is that the Majorana operator is a combination of fermion creation and annihilation operators and hence breaks charge conservation symmetry. This is related to the fact that the Majorana chain model we are going to study breaks charge conservation symmetry and is a superconductor.

   The Hamiltonian of the Majorana chain is, in the exactly solvable limit

   $$H_{MC} = \sum_k i\gamma_{2k}\gamma_{2k+1} \tag{41}$$

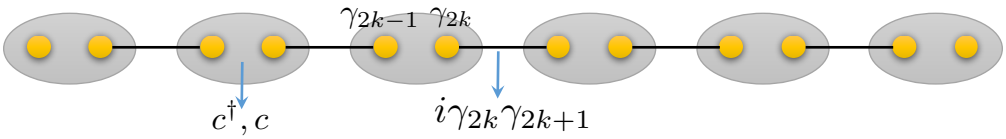

Figure 7: The Majorana chain model: each lattice site contains a fermion mode which can be decomposed into two Majorana modes. The Majorana modes couple to another one on a nearest neighbor site, leaving one Majorana modes at each end of an open chain, giving rise to a two fold degeneracy.

That is, every Majorana mode is coupled to another one on a neighboring lattice site, as shown in Fig.7. This form of coupling is similar to that of the Haldane chain shown in Fig.1. If we recombine the coupled Majorana modes into a fermion mode as $b_k^\dagger = \frac{\gamma_{2k}+i\gamma_{2k+1}}{2}$, $b_k = \frac{\gamma_{2k}-i\gamma_{2k+1}}{2}$, then the Hamiltonian becomes

$$H_{MC} = \sum_k (1 - 2b_k^\dagger b_k) \tag{42}$$

That is, the new fermion modes decouple in the Hamiltonian and in the ground state they are filled.

The interesting feature of this model again shows up on the boundary which holds isolated Majorana modes γ_1, γ_{2N} that are not coupled to anything. These two modes give rise to the two fold ground state degeneracy in an open chain. This Majorana edge mode is similar to the spin 1/2 edge mode of the Haldane chain, but also different in that each Majorana mode does not form an independent Hilbert space and the two fold degeneracy does not need protection of symmetry. In a fermion system, in which the fermion parity symmetry is always preserved, this two fold ground state degeneracy is stable to all kinds of perturbation.

3. In 2D, we talked about the topological insulator – the quantum spin Hall effect. There is also a topological superconductor which can be obtained from a similar construction. That is, one can take one copy of $p+ip$ superconductor for spin up and one copy of $p-ip$ superconductor for spin down and stack them together. The boundary of the system would host a left moving Majorana mode with spin up and a right moving Majorana mode with spin down. When time reversal symmetry is respected, this helical Majorana edge mode cannot be removed.

4. There are many different SPT phases in strongly interacting boson systems as well. One particularly interesting one is the bosonic integer quantum Hall system[25]. Unlike fermions, bosons do not fill Landau levels. To have an integer quantum Hall effect in boson system, the bosons have to interact very strongly. In particular, one can imagine having two species of bosons in a magnetic field each with filling fraction one. Their interaction is such that one species sees the other species as a vortex. In this way, the system can have quantized EM Hall response with $\sigma_{xy} = 2e^2/h$. On the other hand, this is a symmetry protected phase, in the sense that the nontrivial feature is only present if the charge conservation symmetry of the system is preserved. If charge conservation is broken, then the topological order becomes trivial. In particular, this implies that unlike the fermionic integer quantum Hall system, the thermal Hall conductance of the system is zero (no matter whether charge conservation is preserved or not). In [22], it was shown numerically that this kind of order can be realized with two-body delta interaction among the bosons.

   The difference between the fermionic and boson integer quantum Hall effect can be understood from their edge mode structure. As shown in Fig.8, the fermionic integer quantum Hall system

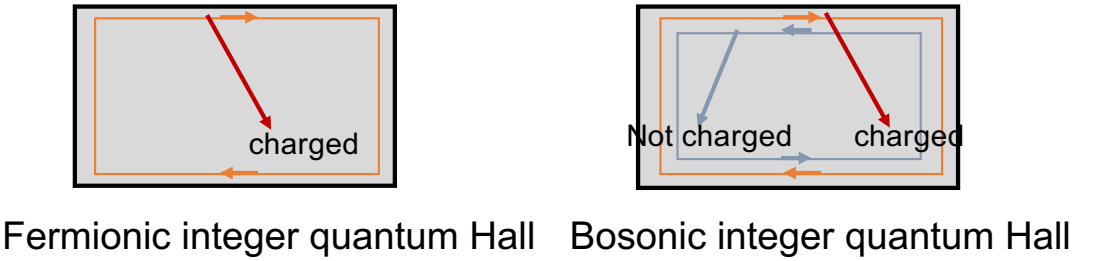

Figure 8: Fermionic vs. bosonic integer quantum Hall effect, difference in edge structure.

hosts a chiral conducting channel which carries both energy and charge. Therefore, both the EM and thermal Hall conductance are nonzero. The bosonic integer quantum Hall system on the other hand hosts two edge modes, a clockwise one carrying both charge and energy and a counter-clockwise one carrying only energy but not charge. Therefore, the EM Hall conductance is nonzero but the thermal Hall conductance is zero.

5. 3D topological insulators[8, 20, 23, 11, 12, 6] and topological superconductors are most prominent examples of SPT phases in 3D. They host gapless Dirac and Majorana cones respectively on their surface, where the spin winds around the cone as shown in Fig.9 (figure taken from [12]).

   Another interesting feature of 3D SPT phases is that the boundary can be gapped and symmetric at the same time. While this is not possible on the 1D boundary of 2D SPTs, the 2D boundary of 3D SPT phases can develop topological order and remove gapless excitation without breaking symmetry. The nontrivial-ness of the boundary state is then encoded in the way the fractional excitations of the topological phase transform under the global symmetry. Just like a single Dirac cone cannot appear in a pure 2D systems with time reversal symmetry but can appear on the surface of a 3D TI, the topological order that appears on the surface of a 3D SPT phase is anomalous and cannot exist in purely 2D systems. This possibility has been explored in various 3D SPT phases, including the fermionic and bosonic topological insulator, topological superconductor and topological crystalline insulators[27, 29, 3, 2, 28, 4, 19, 7, 13, 10].

References

[1] I. Affleck, T. Kennedy, E. H. Lieb, and H. Tasaki. Rigorous results on valence-bond ground states in antiferromagnets. *Phys. Rev. Lett.*, 59(7):799–802, Aug. 1987.

[2] P. Bonderson, C. Nayak, and X.-L. Qi. A time-reversal invariant topological phase at the surface of a 3d topological insulator. *Journal of Statistical Mechanics: Theory and Experiment*, 2013(09):P09016, 2013.

[3] F. J. Burnell, X. Chen, L. Fidkowski, and A. Vishwanath. Exactly soluble model of a three-dimensional symmetry-protected topological phase of bosons with surface topological order. *Phys. Rev. B*, 90:245122, Dec 2014.

[4] X. Chen, L. Fidkowski, and A. Vishwanath. Symmetry enforced non-abelian topological order at the surface of a topological insulator. *Phys. Rev. B*, 89:165132, Apr 2014.

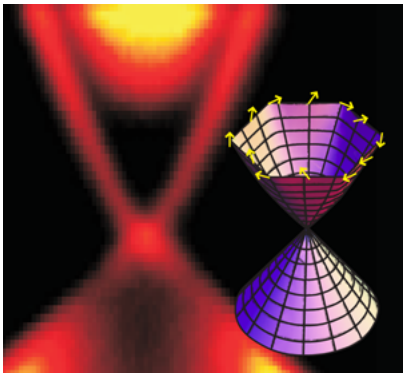

Figure 9: Dirac cone on the surface of a 3D topological insulator.

[5] X. Chen, Z.-C. Gu, and X.-G. Wen. Classification of gapped symmetric phases in one-dimensional spin systems. *Phys. Rev. B*, 83(3):035107–, Jan. 2011.

[6] Y. L. Chen, J. G. Analytis, J.-H. Chu, Z. K. Liu, S.-K. Mo, X. L. Qi, H. J. Zhang, D. H. Lu, X. Dai, Z. Fang, S. C. Zhang, I. R. Fisher, Z. Hussain, and Z.-X. Shen. Experimental realization of a three-dimensional topological insulator, bi2te3. *Science*, 325(5937):178–181, 2009.

[7] L. Fidkowski, X. Chen, and A. Vishwanath. Non-abelian topological order on the surface of a 3d topological superconductor from an exactly solved model. *Phys. Rev. X*, 3:041016, Nov 2013.

[8] L. Fu, C. L. Kane, and E. J. Mele. Topological insulators in three dimensions. *Phys. Rev. Lett.*, 98(10):106803–, Mar. 2007.

[9] F. D. M. Haldane. Continuum dynamics of the 1-D heisenberg antiferromagnet: Identification with the O(3) nonlinear sigma model. *Physics Letters A*, 93:464, 1983.

[10] M. Hermele and X. Chen. Bosonic topological crystalline insulators and anomalous symmetry fractionalization via the flux-fusion anomaly test. *to appear*, 2015.

[11] D. Hsieh, D. Qian, L. Wray, Y. Xia, Y. S. Hor, R. J. Cava, and M. Z. Hasan. A topological dirac insulator in a quantum spin hall phase. *Nature*, 452(7190):970–974, Apr. 2008.

[12] D. Hsieh, Y. Xia, D. Qian, L. Wray, J. H. Dil, F. Meier, J. Osterwalder, L. Patthey, J. G. Checkelsky, N. P. Ong, A. V. Fedorov, H. Lin, A. Bansil, D. Grauer, Y. S. Hor, R. J. Cava, and M. Z. Hasan. A tunable topological insulator in the spin helical dirac transport regime. *Nature*, 460(7259):1101–1105, July 2009.

[13] H. Isobe and L. Fu. Theory of interacting topological crystalline insulators. *Phys. Rev. B*, 92:081304, Aug 2015.

[14] C. L. Kane and E. J. Mele. Quantum spin hall effect in graphene. *Phys. Rev. Lett.*, 95(22):226801–, Nov. 2005.

[15] C. L. Kane and E. J. Mele. z_2 topological order and the quantum spin hall effect. *Phys. Rev. Lett.*, 95(14):146802–, Sept. 2005.

[16] A. Y. Kitaev. Unpaired majorana fermions in quantum wires. *PhysicsUspekhi*, 44(10S):131–136, 2001.

[17] M. König, S. Wiedmann, C. Brüne, A. Roth, H. Buhmann, L. W. Molenkamp, X.-L. Qi, and S.-C. Zhang. Quantum spin hall insulator state in HgTe quantum wells. *Science*, 318(5851):766–770, Nov. 2007.

[18] M. Levin and Z.-C. Gu. Braiding statistics approach to symmetry-protected topological phases. *Phys. Rev. B*, 86:115109, Sep 2012.

[19] M. A. Metlitski, C. L. Kane, and M. P. A. Fisher. Symmetry-respecting topologically ordered surface phase of three-dimensional electron topological insulators. *Phys. Rev. B*, 92:125111, Sep 2015.

[20] J. E. Moore and L. Balents. Topological invariants of time-reversal-invariant band structures. *Phys. Rev. B*, 75(12):121306–, Mar. 2007.

[21] F. Pollmann, A. M. Turner, E. Berg, and M. Oshikawa. Entanglement spectrum of a topological phase in one dimension. *Phys. Rev. B*, 81:064439, Feb 2010.

[22] N. Regnault and T. Senthil. Microscopic model for the boson integer quantum hall effect. *Phys. Rev. B*, 88:161106, Oct 2013.

[23] R. Roy. Topological phases and the quantum spin hall effect in three dimensions. *Phys. Rev. B*, 79(19):195322–, May 2009.

[24] N. Schuch, D. Perez-Garcia, and I. Cirac. Classifying quantum phases using matrix product states and projected entangled pair states. *Phys. Rev. B*, 84:165139, Oct 2011.

[25] T. Senthil and M. Levin. Integer quantum hall effect for bosons: A physical realization. *ArXiv e-print 1206.1604*, June 2012.

[26] A. M. Turner, F. Pollmann, and E. Berg. Topological phases of one-dimensional fermions: An entanglement point of view. *Phys. Rev. B*, 83(7):075102–, Feb. 2011.

[27] A. Vishwanath and T. Senthil. Physics of three-dimensional bosonic topological insulators: Surface-deconfined criticality and quantized magnetoelectric effect. *Phys. Rev. X*, 3:011016, Feb 2013.

[28] C. Wang, A. C. Potter, and T. Senthil. Gapped symmetry preserving surface state for the electron topological insulator. *Phys. Rev. B*, 88:115137, Sep 2013.

[29] C. Wang and T. Senthil. Boson topological insulators: A window into highly entangled quantum phases. *arXiv:1302.6234*, 2013.